Excited-State Structure and Dynamics in FMO Antenna Complexes from Photosynthetic Green Sulfur Bacteria

Simone I. E. Vulto,* Sieglinde Neerken, Robert J. W. Louwe, Michiel A. de Baat, Jan Amesz, and Thijs J. Aartsma

Department of Biophysics, Huygens Laboratory, Leiden University, P.O. Box 9504, 2300 RA Leiden, The Netherlands

Received: July 13, 1998; In Final Form: October 1, 1998

Absorption difference spectra for the singlet excited states of the Fenna−Matthews−Olson (FMO) complex from the green sulfur bacteria *Prosthecochloris aestuarii* and *Chlorobium tepidum* were simulated by exciton theory. The same assumptions and parameters were used as applied earlier (Louwe, R. J. W.; Vrieze, J.; Hoff, A. J.; Aartsma, T. J. *J. Phys. Chem. B* **1997**, *101*, 11280. Vulto, S. I. E.; de Baat, M. A.; Louwe, R. J. W.; Permentier, H. P.; Neef, T.; Miller, M.; van Amerongen, H.; Aartsma, T. J. *J. Phys. Chem. B* **1998**, *102*, 9577). The difference spectra show a bleaching near the wavelength of excitation, due to ground-state bleaching and stimulated emission. Additional negative and positive bands reflect changes in interaction with other bacteriochlorophylls than the one that is mainly excited at the transition frequency. Simulated spectra were compared with experimental difference spectra obtained by pump−probe experiments in the femto- and picosecond time region with excitation pulses in the spectral range 800−828 nm. In general, good agreement was obtained. Various difference spectra developed during the first 1 to 2 ps, but in all cases the system relaxed to the lowest energy state, which was largely completed in 10 ps.

Introduction

The Fenna−Matthew−Olson (FMO) complex of *Prosthecochloris (P.) aestuarii* was the first photosynthetic pigment−protein complex of which the structure was determined by X-ray crystallography.[1,2] Last year, also the structure of the FMO complex of another green sulfur bacterium, *Chlorobium (C.) tepidum*, was solved.[3] Both complexes consist of an arrangement of three identical subunits, with a 3-fold rotational symmetry axis. Each subunit contains seven bacteriochlorophylls (BChls) *a*, which gives a total of 21 pigments for the entire complex. The nearest-neighbor distances (center-to-center) within one subunit vary from 11 to 14 Å, while the distance between nearest neighbors in different subunits of the trimer is about 24 Å. Only minor differences were found in the positions and orientations of the various BChls in the FMO complexes of both species. Nevertheless, the low-temperature optical spectra showed significant differences.[4,5] This indicated that the local environment and thus the site energies of corresponding individual BChls in the two complexes differ considerably from each other, in line with the fact that the amino acid sequences show only 78% homology.[6]

During the past decades various attempts have been made to model the optical spectra of the FMO complex on the basis of its three-dimensional structure.[7−12] These attempts met with limited success only, but recently, in two publications from our laboratory,[5,13] it was shown that a good agreement could be obtained with the experimental spectra when the interaction energies between the BChls were taken to be lower than those used in the earlier attempts. This applied to the FMO complexes of both species.

In this publication, we report on a simulation of absorbance difference spectra of the singlet excited states of the FMO complexes from *P. aestuarii* and *C. tepidum*, using the same assumptions as applied earlier. The absorbance difference spectra are obtained from an exciton model and assuming that only one excitation was present in the complex. Significant differences between the spectra corresponding to the different steps in the relaxation process are observed. The calculated spectra are characterized by multiple peaks due to ground-state bleaching, stimulated emission, and excited-state absorption. In general, the difference spectra showed maximal bleaching near the wavelength of excitation. When compared with experimental data, such difference spectra provide very sensitive tests for the accuracy of the simulations. A quite satisfactory agreement with the experimental spectra was obtained in pump−probe measurements at low temperature. Monitoring the time evolution of the difference spectra gave information on the rates and pathways of relaxation in the complexes.

Experimental Section

Simulations. Parameters for the description of the electronic structures of the one-exciton states, i.e., the site energies of and the dipole−dipole interactions between the various BChls in the FMO complexes from *P. aestuarii* and *C. tepidum*, were taken from refs 13 and 5, respectively. The exciton simulations were based on the following assumptions:[13] (i) only interactions within a single subunit are significant, (ii) the effective dipole strength in calculating the interaction energies is equal to 28.7 D^2, and (iii) BChl 3, according to the numbering of Fenna and Matthews,[1] was taken to be the lowest energy molecule. Q_y-dipole moments of the individual BChls were assumed to be oriented parallel to the axis running through the N_I and N_{III} nitrogen atoms. The atomic coordinates of the FMO complexes from both species were obtained from the Brookhaven Protein Databank. Using these parameters, the two-exciton-state energy

* Corresponding author. Fax: 31-71 5275819. E-mail: vulto@biophys.leidenuniv.nl.

10.1021/jp983003v CCC: $15.00
Published on Web 12/01/1998

levels together with the corresponding oscillator strengths were calculated as described in, e.g., refs 14−16. When the calculated energies and the oscillator strengths for transitions from the ground to the one-exciton and from the one-exciton to the two-exciton state are combined, the absorbance difference spectrum for each state was calculated according to

$$\Delta A(\lambda,i) = -\mathrm{ABS}(\lambda) - \mathrm{SE}(\lambda,i) + \mathrm{ESA}(\lambda,i)$$

where $\Delta A(\lambda,i)$ is the absorbance difference spectrum for the ith state, ABS(λ) is the absorption spectrum of the ground state, SE(λ,i) is the stimulated emission from the ith excited state, and ESA(λ,i) is the absorption spectrum of the transition from the ith state to the two-exciton state. In this calculation, it was assumed that only one of the exciton states was occupied at a time. Since the Einstein coefficients for stimulated emission and absorption are equal, it was assumed that the spectrum of the stimulated emission was equal to the absorption spectrum for the ith state; that is, the fluorescence Stokes shift was neglected. This is justified by the weak electron−phonon coupling of the optical transitions in the FMO complex.[17−19] For the 825 nm band in *P. aestuarii*, the fluorescence Stokes shift is less than 3 nm at low temperature.[20] To each transition, both from the ground to the one-exciton state and from the one- to the two-exciton state, a Gaussian band was assigned with a width of 80 cm^{-1} at half-maximum. This implies that lifetime broadening effects are neglected in the simulations of the spectra.

Laser System. Time-resolved transient absorption measurements were performed with a home-built amplified dye laser system with continuum generation and optical multichannel analyzer (OMA) detection, operating at 10 Hz, described by Kennis et al. [21,22] The time resolution was 300 fs. Wavelength-selective excitation pulses were obtained by passing the continuum pulse through an amplified dye cell (pumped by a frequency-doubled, Q-switched Nd:YAG laser) and subsequently through a suitable interference filter with a bandwidth of 6−10 nm (Ferroperm, CVI). The dye LDS 821 (Exciton) was used for amplification. The probe pulse was polarized at the magic angle with respect to the pump. At each delay, 3000−5000 spectra were recorded and averaged. Per pulse, about 0.5% of the bacteriochlorophylls were excited; therefore, annihilation effects could be ignored. We corrected for the group velocity dispersion by applying a third-order polynomial function that was obtained by measuring the dispersion in CS_2.[23,24] All measurements were performed at 10 K in a helium flow cryostat (Utreks-LSO, Estonia).

Sample Preparation. The FMO complexes of both *P. aestuarii* and *C. tepidum* were isolated as described by Francke and Amesz[4] and dissolved in 50 mM Tris/HCl and 200 mM sodium chloride (pH 8.3). To obtain a clear glass upon cooling, 66% (v/v) glycerol was added. The samples were contained in a 0.5 mm cuvette and adjusted to an absorbance of 0.5 at 809 nm at room temperature.

Results and Discussion

Simulations. Absorption spectra at 10 K of the FMO complexes from *P. aestuarii* and *C. tepidum* are shown in Figure 1. As noted earlier,[4] the two spectra are not identical; the spectrum of *P. aestuarii* has a maximum absorption at 815 nm, while the spectrum of *C. tepidum* has its maximum at 806 nm. For both species, the electronic structure of the one-exciton state has been described successfully by simulating the various optical spectra (absorption, circular dichroism, linear dichroism, triplet-minus-singlet) by means of exciton theory.[5,13] The corresponding transitions in the simulated absorption spectra are also shown

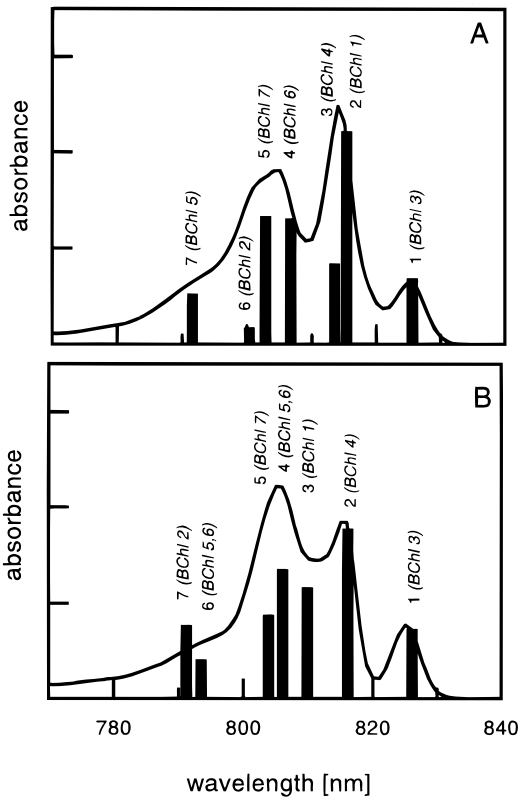

Figure 1. Absorption spectra of the FMO complexes from the green sulfur bacteria (A) *P. aestuarii* and (B) *C. tepidum* at 10 K. Both spectra are normalized to the same area. The electronic structure of the exciton manifold as calculated by Louwe et al.[13] for *P. aestuarii* and by Vulto et al.[5] for *C. tepidum* is indicated by sticks. Each stick represents a certain energy level, with the height being proportional to the oscillator strength of that transition. Each stick is assigned with a number in order of increasing energy, and in parentheses, the BChl is indicated that has the largest contribution to the oscillator strength of that state (the BChls are numbered according to Fenna and Matthews[1]).

in Figure 1. For each complex, the seven exciton states were numbered 1−7 in order of increasing energy,[5] and this notation will be used throughout this paper too. The lowest states of the Q_y-exciton manifold in the FMO complexes from both *P. aestuarii* and *C. tepidum* have equal energies and are mainly determined by the contribution of BChl 3. However, there are significant differences in other energy levels; for example, state 2 corresponds mainly to BChl 1 in *P. aestuarii* but to BChl 4 in *C. tepidum*. In *P. aestuarii*, the 815 nm band in the absorption spectrum results from two exciton states, 2 and 3 (mainly BChls 1 and 4), whereas in *C. tepidum* only state 2 (mainly BChl 4) is involved.

The similarities and differences in electronic structure are also reflected in the simulated ΔA spectra. The spectra were calculated with the assumption that only a single exciton state was populated. For the lowest energy state (state 1, with main contribution from BChl 3) of the FMO complex of *P. aestuarii*, this is illustrated in Figure 2. It is quite clear that not all transitions gain equal oscillator strength, especially not for the excited-state absorption, where 21 transitions ($N(N-1)/2$) are in principle possible. The difference spectrum is characterized by multiple peaks with different amplitudes and signs. The largest peak, the negative band at 825 nm, is caused by ground-state bleaching and stimulated emission at the transition frequency. However, peaks (positive as well as negative) at shorter wavelengths are also observed as is typical for a strongly coupled system.

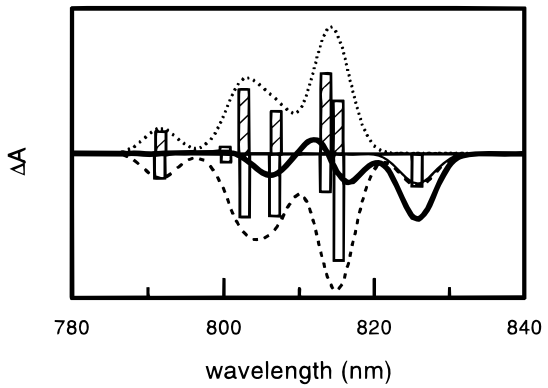

Figure 2. Absorbance difference spectrum of the FMO complex from *P. aestuarii* (thick solid line) for the transition to state 1 (the lowest energy level), as calculated from the ground-state bleaching (dashed), the excited-state absorption (dotted), and the spectrum of the stimulated emission (thin solid line), as described in the text. Sticks denote the transitions for ground-state (open) and excited-state absorption (hatched).

The absorbance difference spectra for each of the seven exciton states of the FMO complexes from both species are shown in Figure 3. In most cases, the largest peak is a bleaching at the transition frequency, but, as for the difference spectrum of Figure 2, this negative band is always accompanied by other bands at shorter or longer wavelengths. The ΔA spectrum of state 1 in *C. tepidum* is very similar to the corresponding one in *P. aestuarii*. This could be expected since for both species this state has about the same energy and is mainly determined by BChl 3. The same is true for state 5, which is mainly determined by BChl 7 in both complexes, but here the differences are a little larger.

Experiments. As illustrated in Figure 2, the absorbance difference spectra are sensitive indicators of the validity of our model calculations. It was therefore of interest to test our results experimentally by measuring pulse-induced spectra in pump−probe experiments. Such spectra are shown in Figures 4 and 5 for the two species for various wavelengths of excitation and at various times after the pulse.

The spectra obtained at 10 ps after the excitation pulse (dotted lines) are all similar, with a maximum bleaching near 826 nm, and for both species, they resemble the calculated spectra of state 1. This indicates that, independent of the wavelength of excitation, the FMO complexes have largely relaxed to the lowest energy level within 10 ps, in agreement with kinetic measurements at selected wavelengths.[25,26] Similar difference spectra have been measured recently for the *C. tepidum* FMO complex by Buck et al.[14] at 80 ps and by Freiberg et al.[27] at 5 ps delay.

It thus appears that our simulations of the state 1 difference spectra give satisfactory fits of the experimental spectra of the *P. aestuarii* as well as of the *C. tepidum* FMO complex. A puzzling observation, however, is the variability of the relative amplitudes of the bands in the "final" experimental spectra, which for both FMO complexes appear to depend on the excitation wavelength. The 815 nm band is highest upon excitation near 815 nm, as seen in Figures 4C and 5C, while the 825 nm band dominates upon excitation at 827 or 828 nm. The 804 nm band is particularly strong upon excitation at 800 and 806 nm, as is most clearly seen in Figure 4B. It is unlikely that these effects reflect impurities since they occur with both FMO complexes. We did not attempt to study this phenomenon at times longer than 10 ps and therefore cannot exclude that it represents a slow phase in the relaxation process. It may be remarked that similar observations were reported recently for reaction centers of purple bacteria[28] and were attributed to incomplete relaxation on a picosecond time scale.

Whereas the "final" experimental difference spectra reflect the spectrum of state 1, another test for the validity of our simulations can be performed in principle by comparing the simulated difference spectra with those measured immediately after the excitation, i.e., before relaxation to lower energy levels has occurred. One should, however, realize that not all of the difference spectra of Figure 3 can be checked experimentally in this way. For the *P. aestuarii* protein, such a check is limited to transitions to states 1, 2, and 5, corresponding to BChls 3, 1, and 7, respectively (see Figures 1 and 3). Transitions to states

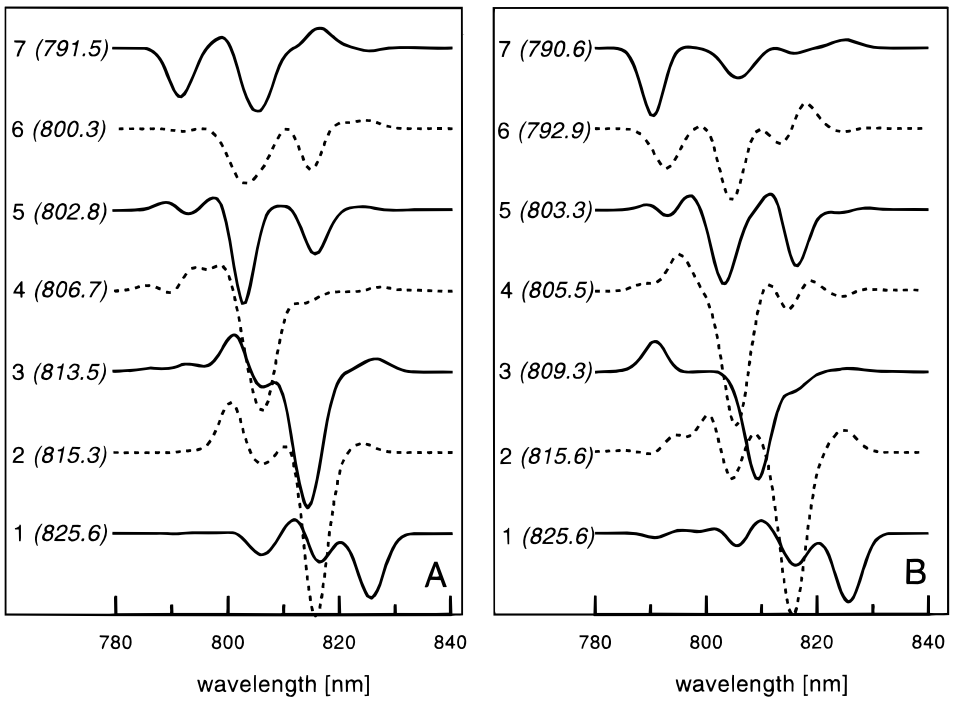

Figure 3. Calculated absorbance difference spectra for the FMO complexes of (A) *P. aestuarii* and (B) *C. tepidum* upon excitation in each of the seven transitions to the one-exciton state at the indicated wavelengths. It was assumed that only one level is populated in time.

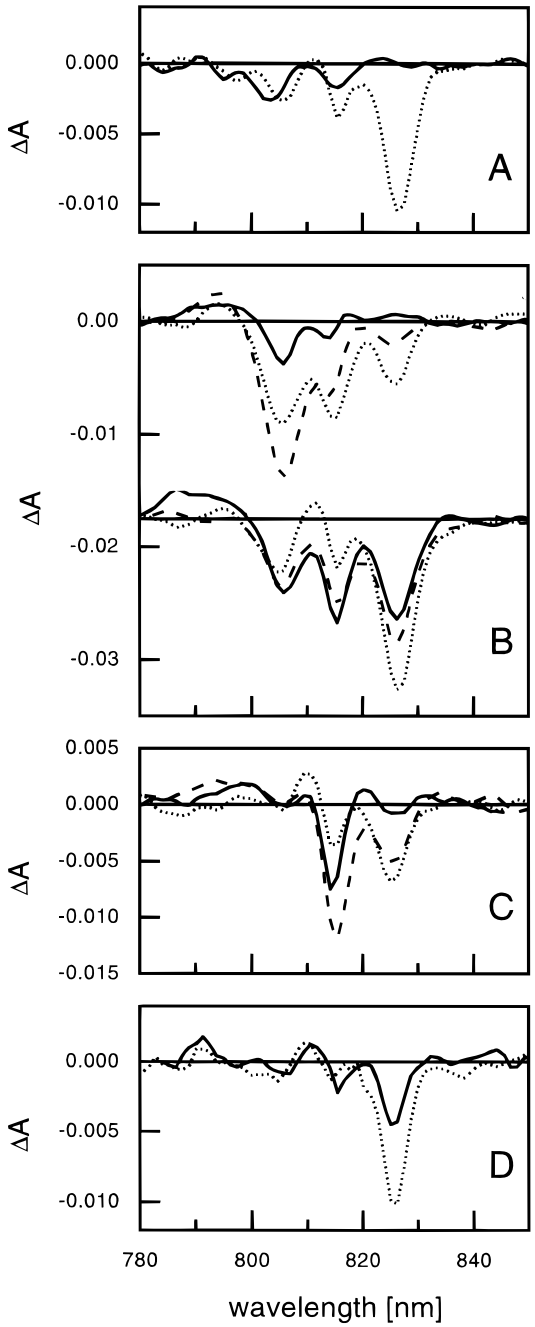

Figure 4. Time-resolved absorbance difference spectra of the FMO complex from *P. aestuarii* at 10 K: (A) excitation at 800 nm, spectra were recorded at 0 (solid) and 10 ps (dotted) after the pulse; (B) excitation at 806 nm, spectra recorded at 0 (solid), 0.4 (dashed), and 0.8 ps (dotted) delay, spectra at 1.1 (solid), 1.7 (dashed), and 10 ps (dotted) delay are shifted by −0.017 units of absorbance; (C) excitation at 814 nm, recorded at 0 (solid), 0.8 (dashed), and 10 ps (dotted) delay; (D) excitation at 828 nm with spectra recorded at 0 (solid) and 10 ps (dotted) delay.

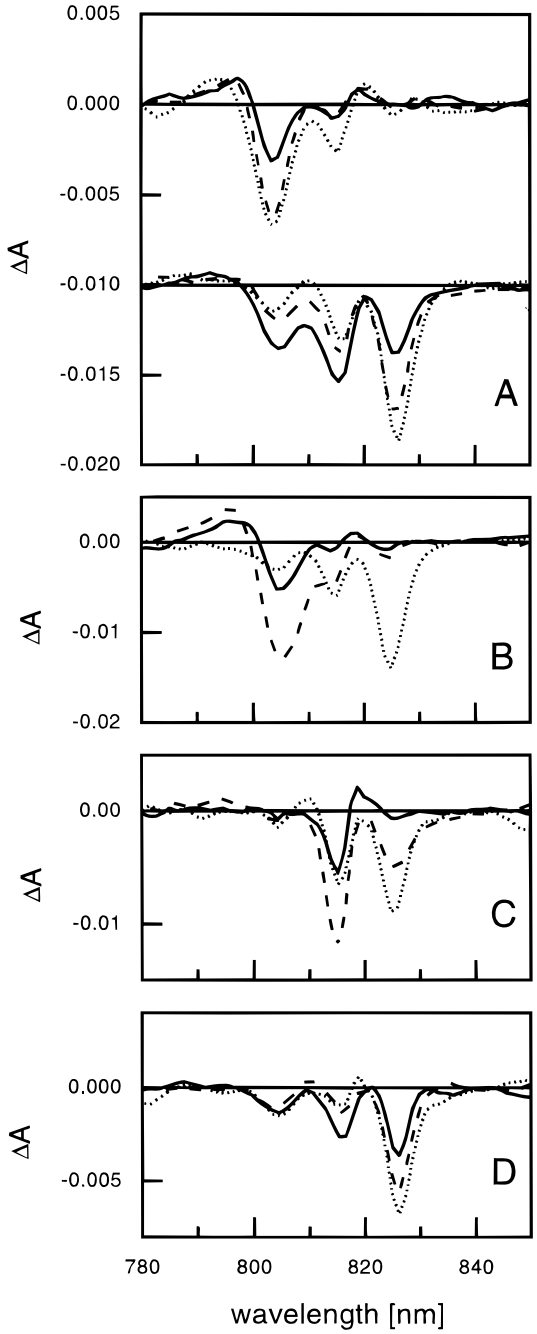

Figure 5. Time-resolved absorbance difference spectra of the FMO complex from *C. tepidum* at 10 K: (A) excitation at 800 nm, spectra were recorded at 0 (solid), 0.1 (dashed), and 0.3 ps (dotted) after the pulse, spectra at delays of 0.7 (solid), 1.6 (dashed), and 10 ps (dotted) are shifted by −0.01; (B) excitation at 807 nm, recorded at 0 (solid), 0.3 (dashed), and 10 ps (dotted) delay; (C) excitation at 817 nm, recorded at 0 (solid), 0.7 (dashed), and 10 ps (dotted) after the excitation; (D) excitation at 827 nm with spectra recorded at 0 (solid), 0.2 (dashed), and 10 ps (dotted) delay.

3 and 6 are too weak, while the transition to state 4 has too much overlap with other transitions and cannot be excited preferentially. For the transition to state 7, the lifetime of the initially excited state (<100 fs[25]) is too short in relation to our time resolution. For *C. tepidum* mainly the transitions to states 1, 2, and 4 are experimentally accessible.

Figure 6 shows the absorbance difference spectra calculated for excitation at various wavelengths between 790 and 830 nm. The relative populations of the various states (at time zero) were calculated for each excitation pulse, taking into account its spectral profile. The spectra were then obtained by linear combinations of the difference spectra of Figure 3. A pulse at 826 or 828 nm populates mainly state 1 in both FMO complexes. State 2 dominates at 814 (*P. aestuarii*) or 817 nm (*C. tepidum*), whereas mainly states 4 and 5 are excited upon excitation at 800−807 nm. If we compare those spectra with the experimentally obtained initial spectra (Figure 6, dashed lines), we observe, in general, a quite satisfactory agreement. Results for *P. aestuarii* are shown in Figure 6A. The initial spectrum obtained upon excitation at 800 nm shows negative bands at 804 and 815 nm,

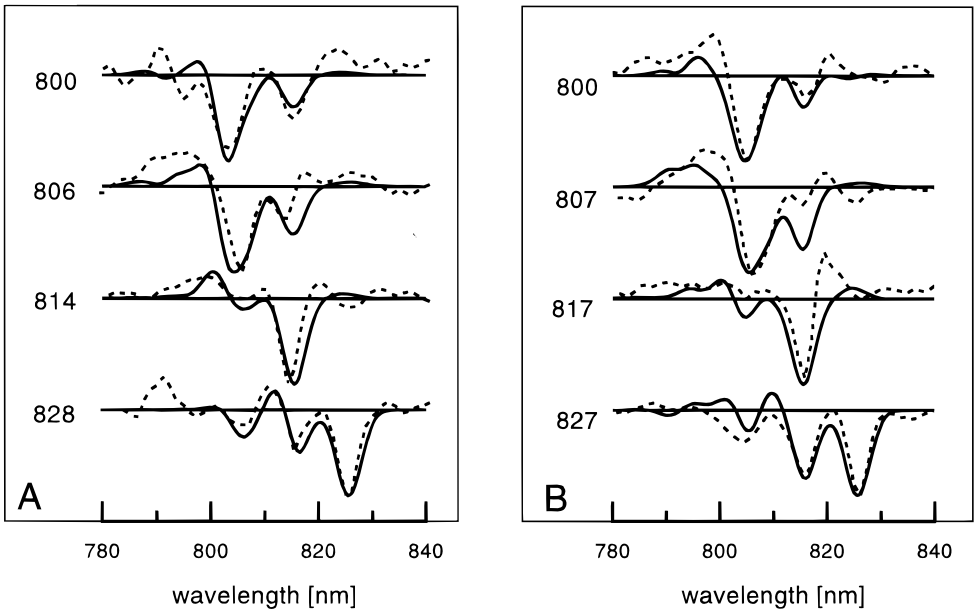

Figure 6. Measured initial absorbance difference spectra (dashed) of (A) *P. aestuarii* and (B) *C. tepidum* upon excitation at the indicated wavelengths. These spectra are taken from Figures 4 and 5. The solid lines give the calculated initial spectra, taking into account the spectral profile of the excitation pulse (see text).

in excellent agreement with the simulated spectrum. The weak positive band near 800 nm in the simulated spectrum is not observed in the experimental one. This band was clearly visible, however, upon excitation at 806 nm, while negative bands appeared at 806 and 815 nm, the latter being relatively weak in this case. For excitation at 814 nm, the agreement is satisfactory too. Finally, excitation at 828 nm induced a state 1 type of spectrum, as mentioned already. Our simulations clearly fit the experimental data better than do those of Buck et al.[14] The latter were based on the so-called OKT set of parameters,[11] which have already been shown[13] to give less satisfactory simulations of the optical spectra.

For *C. tepidum* (Figure 6B), the correspondence between model and experiment was quite good upon excitation at 800 nm, with a main negative band at 804 nm, a minor one at 815 nm, and excited-state absorption at 797 nm. A good match was also obtained with excitation at 807 nm, although, as in *P. aestuarii*, the negative band at 815 nm was rather weak in the experimental spectrum. The spectrum for 817 nm excitation was strongly dominated by a bleaching band near this wavelength, and this feature is adequately simulated. The initial spectrum with 827 nm excitation agrees quite well with the calculated one; note that the spectrum, with a relatively strong bleaching at 816 nm, deviates from a pure state 1 spectrum, since state 2 is still partially excited at this wavelength.

Figures 4 and 5 also show varying difference spectra obtained at intermediate delay times after the excitation. For the *P. aestuarii* FMO complex, an extensive set of difference spectra, obtained upon excitation at 806 nm, is shown in Figure 4B. The initial spectrum had a main bleaching at 806 nm, but at about 0.4 ps, a change in the spectrum starts to occur with the development of a negative band at 826 nm. According to our simulations (Figure 3), the band at 826 nm can only be due to the lowest energy state, state 1. Thus, our measurements indicate that there is already significant population of this state after a few hundreds of femtoseconds. After about 1.5 ps, this band became the largest one in the difference spectrum, indicating rapid equilibration to the lowest energy state. The band at 815 nm reached a maximum at 1.1 ps and then decreased again. This can be ascribed to the transient population of states 3 and 2, but these two are difficult to distinguish spectroscopically. Again, the kinetics agree with those measured earlier at single wavelengths.[25] Results obtained upon excitation at 814 nm, which is mainly in states 2 and 3, are shown in Figure 4C. After an initial main bleaching at 815 nm, the band at 825 nm developed at the same rate as in the spectra of Figure 4B. As mentioned already, the band at 815 nm did not fully relax to the level of parts A and B of Figure 4, even after 10 ps.

The difference spectra obtained with the *C. tepidum* FMO complex were qualitatively similar to those of the complex from *P. aestuarii*. Figure 5A shows results obtained upon excitation at 800 nm. After an initial bleaching at 804 nm, bands at 815 and 826 nm developed in a similar way as with *P. aestuarii*. If we compare the spectra at 0 and 0.2 ps, it is obvious that the bleaching at 804 nm increases whereas the negative band at 815 nm does not. Only at 0.3 ps, the 815 nm band starts to increase further, and at 0.7 ps, it is the largest band in the difference spectrum. This can be explained by considering the simulated spectra of states 2−5. Apparently the system relaxes first to state 4 (which lacks the 815 nm band) and subsequently to states 3 and 2. The 815 nm band reached a maximum after about 1 ps, followed by a development of the band at 825 nm in less than 2 ps, in agreement with kinetic measurements of Savikhin and Struve at 19 K.[26] Similar results were obtained for excitation at 807 nm (Figure 5B). The spectrum measured at 0.5 ps resembles one measured upon 803 nm excitation by Freiberg et al.[27] Results upon excitation at 817 nm (Figure 5C) were similar to those obtained at 814 nm with *P. aestuarii*. Upon excitation at 826 nm (Figure 5D), a spectrum resembling that of state 1 was formed within 200 fs.

In summary, we conclude that for both FMO complexes excellent agreement is obtained between the calculated and the experimental initial spectra. These results provide additional support for the model of the FMO complex by Louwe et al.[13] This model is based on a description of the optical spectra in terms of point−dipole interactions, and now, it also appears to be able to describe the transitions from the one- to the two-exciton state in the FMO complex. In principle, this information can be used to map the relaxation paths in the manifold of

exciton states of the FMO complex upon optical excitation. This aspect is currently under investigation.

Acknowledgment. This work has been supported by the Life Science Foundation (SLW), financed by The Netherlands Organization for Scientific Research (NWO) and by the EC (Contract FMRX-CT96 0081).

References and Notes

(1) Fenna, R. E.; Matthews, B. W. *Nature* **1975**, *258*, 573.
(2) Tronrud, D. E.; Schmid, M. F.; Matthews, B. W. *J. Mol. Biol.* **1986**, *188*, 443.
(3) Li, Y. F.; Zhou, W.; Blankenship, R. E.; Allen, J. P. *J. Mol. Biol.* **1997**, *271*, 456.
(4) Francke, C.; Amesz, J. *Photosynth. Res.* **1997**, *52*, 137.
(5) Vulto, S. I. E.; de Baat, M. A.; Louwe, R. J. W.; Permentier, H. P.; Neef, T.; Miller, M.; van Amerongen, H.; Aartsma, T. J. *J. Phys. Chem. B* **1998**, *102*, 9577.
(6) Dracheva, S.; Williams, J. C.; Blankenship, R. E. In *Research in Photosynthesis*; Murata, N., Ed.; Kluwer Academic Publishers: Dordrecht, The Netherlands, 1992; p 53.
(7) Pearlstein, R. M.; Hemenger, R. P. *Proc. Natl. Acad. Sci. U.S.A.* **1978**, *75*, 4920.
(8) Pearlstein, R. M. In *Photosynthesis: Energy Conversion by Plants and Bacteria;* Govindjee, Ed.; Academic Press: New York, 1982; p 293.
(9) Pearlstein, R. M. In *Chlorophylls*; Scheer, H., Ed.; CRC Press: Boca Raton, 1991; p 1047.
(10) Pearlstein, R. M. *Photosynth. Res.* **1992**, *31*, 213.
(11) Lu, X.; Pearlstein, R. M. *Photochem. Photobiol.* **1993**, *57*, 86.
(12) Gülen, D. *J. Phys. Chem.* **1996**, *100*, 17683.
(13) Louwe, R. J. W.; Vrieze, J.; Hoff, A. J.; Aartsma, T. J. *J. Phys. Chem. B* **1997**, *101*, 11280.
(14) Buck, D. R.; Savikhin, S.; Struve, W. S. *Biophys. J.* **1997**, *72*, 24.
(15) Spano, F. C. *Phys. Rev. Lett.* **1991**, *67*, 3424.
(16) van Burgel, M.; Wiersma, D. A.; Duppen, K. *J. Chem. Phys.* **1995**, *102*, 20.
(17) Johnson, S. G.; Small, G. J. *J. Phys. Chem.* **1991**, *95*, 471.
(18) Louwe, R. J. W.; Aartsma, T. J. *J. Phys. Chem.* **1997**, *101*, 7221.
(19) Franken, E. M.; Neerken, S.; Amesz, J.; Aartsma, T. J. *Biochemistry* **1998**, *37*, 5046.
(20) Swarthoff, T.; Amesz, J.; Kramer, H. J. M.; Rijgersberg, C. P. *Isr. J. Chem.* **1981**, *21*, 332.
(21) Kennis, J. T. M.; Streltsov, A. M.; Aartsma, T. J.; Nozawa, T.; Amesz, J. *J. Phys. Chem.* **1996**, *100*, 2438.
(22) Kennis, J. T. M.; Streltsov, A. M.; Permentier, H.; Aartsma, T. J.; Amesz, J. *J. Phys. Chem. B* **1997**, *101*, 8369.
(23) Greene, B. J.; Farrow, R. C. *J. Chem. Phys.* **1983**, *98*, 273.
(24) Kennis, J. T. M.; Shkuropatov, A. Y.; van Stokkum, I. H. M.; Gast, P.; Hoff, A. J.; Shuvalov, V. A.; Aartsma, T. J. *Biochemistry* **1997**, *36*, 16231.
(25) Vulto, S. I. E.; Streltsov, A. M.; Aartsma, T. J. *J. Phys. Chem. B* **1997**, *101*, 4845.
(26) Savikhin, S.; Struve, W. S. *Photosynth. Res.* **1996**, *48*, 271.
(27) Freiberg, A.; Lin, S.; Timpmann, K.; Blankenship, R. E. *J. Phys. Chem. B* **1997**, *101*, 7211.
(28) Lin, S.; Taguchi, A. K. W.; Woodbury, N. W. *J. Phys. Chem.* **1996**, *100*, 17067.